Adsorption (2011) 17: 539–550
DOI 10.1007/s10450-010-9319-x

Adsorption of oxygen-containing aromatics used in petrochemical, pharmaceutical and food industries by means of lignin based active carbons

L.M. Cotoruelo · M.D. Marqués · A. Leiva · J. Rodríguez-Mirasol · T. Cordero

Received: 11 August 2010 / Accepted: 30 December 2010 / Published online: 13 January 2011

Abstract The adsorption processes of three aromatic chemicals onto activated carbons (ACs) from aqueous solutions have been studied. Eucalyptus kraft lignin obtained from cellulose industry as a residual biomass has been used to prepare activated carbons by physical activation with CO_2. The influences of the activation time on the surface areas and pore volumes of the ACs were analyzed. The physicochemical properties and the surface chemical structure of the adsorbents have been studied by means of N_2 and CO_2 adsorption, ultimate analysis, XPS, TPD and SEM. XPS and TPD spectra of the ACs have suggested the presence of aromatic rings and carbon-oxygen functional groups in the solid surfaces. The potential use of the ACs for the removal of acetaminophen (paracetamol), salicylic acid and benzoic acid has been investigated at different pH, temperature and contact time. The adsorption equilibrium data have been correlated to Langmuir isotherm model. The thermodynamic study has been developed, the values of ΔH, ΔG, and ΔS have been calculated and they indicated that the processes are endothermic for acetaminophen and exothermic for salicylic and benzoic acids. The analysis of the kinetic experiments showed that the effective diffusivities are low; 10^{-12} to 10^{-11} cm^2/s, and they are the corresponding to intraparticle mass transfer, which appears as the controlling step for the net adsorption processes.

Keywords Lignin · Aromatic compounds · Activated carbons · Adsorption · Isotherm

L.M. Cotoruelo (✉) · M.D. Marqués · A. Leiva · J. Rodríguez-Mirasol · T. Cordero
Departamento de Ingeniería Química, Facultad de Ciencias, Universidad de Málaga, 29071 Málaga, España
e-mail: lcot@uma.es

1 Introduction

Aqueous-phase adsorption is one of the most efficient methods for the removal of colours, odours, and organic micropollutants in general, from process or refused effluents.

During the last years, we have developed several procedures for the preparation of activated carbons from lignocellulosic wastes (Tancredi et al. 1996; González-Serrano et al. 1997; Márquez-Montesino et al. 2001). One possibility has been the use of eucalyptus kraft lignin as raw material; which includes its carbonization and partial gasification with CO_2 (Rodríguez-Mirasol et al. 1993a, 1993b). The activated carbons (ACs) obtained and classified according to different series have been used as adsorbents for the separation of selected organic compounds from their aqueous solutions. The chemical nature of the AC surface and its porous structure determine the rate and the final adsorption capacity. Those result from the preparation conditions. Simple aromatic hydrocarbons (benzene and toluene) and some of their substituted compounds, as chlorinated, phenolic, and nitroproducts (nitro and amino) have been tested as adsorbates (Cotoruelo et al. 2007a, 2007b). The chemical nature, solubility, dissociation grade in solution and molecular size, are the determining properties of the adsorbates. Operative variables as temperature, pH, adsorbent dose and adsorbate concentration, define the equilibrium systems, with their adsorption isotherms and the corresponding thermodynamic parameters (ΔH, ΔG, ΔS). On the other hand, the kinetic studies provide the data (mass transfer parameters) on the adsorption rate control, and they give helpful information to design the adsorbers at the high scale applications. In the present work, three activated carbons prepared from eucalyptus kraft lignin by physical activation were studied for their use as adsorbents. Three aromatic compounds with oxygen-containing functional groups in their molecules

have been selected as adsorbates: paracetamol (PA), benzoic acid (BA), and salicylic acid (SA). Their molecules include carbonyl, carboxyl, and hydroxyl groups. The three selected adsorbates are widely used as intermediates or final products in petrochemical, pharmaceutical and food industries. For this reason, their undesirable appearance in different fluid streams is highly probable, being their separation/removal a necessary step of technical, environmental or economical concerns. There is a variety of works about aqueous-phase adsorption of PA, BA, and SA, onto adsorbent materials, as activated carbons, carbon cloths, and polymeric resins, among others (Oda et al. 1981; Shirgaonkar et al. 1992; Mazet et al. 1994; Brasquet et al. 1997; Koh and Nakajima 2000; Franz et al. 2000; Ania et al. 2002a, 2002b; Terzyk et al. 2003; Otero et al. 2005; Ayranci et al. 2005; Ayranci and Duman 2006; Khenniche and Aissani 2009).

2 Materials and methods

2.1 Adsorbents preparation

The eucalyptus kraft lignin was supplied by the Empresa Nacional de Celulosas (Spain). The starting lignin has high content in inorganic matter (∼12% ash), so it was previously treated by predevolatilization at 623 K under N_2 atmosphere for 2 h. The resulting precarbonized material was washed with H_2SO_4 (5% w/w) aqueous solution until its final ash content. This precarbonized substrate was carbonized under N_2 atmosphere in a horizontal tubular furnace. The heating rate was 10 K/min until 823 K, temperature that was held for 2 h. The activation has been carried out by CO_2 partial gasification at 1073 K for different reaction times to obtain a series of ACs with different burn off (Rodríguez-Mirasol et al. 1993a, 1993b). The abbreviated name of each sample is referred to the activation time (h): A4, A12 and A20.

The porous structures of the ACs were characterized by means of adsorption-desorption of N_2 at 77 K and CO_2 at 273 K using a Quantachrome apparatus (Autosorb-1 model), and by mercury porosimetry using a Carlo Erba mercury Porosimeter 4000. N_2 adsorption was used to calculate the apparent surface area (A_{BET}), external area (A_S), the micropore ($d < 2$ nm), and the narrow mesopore (2 nm $< d <$ 8 nm) volumes. CO_2 adsorption was used to calculate the narrow micropore by applying the Dubinin-Radushkevich equation. Mercury porosimetry was used to calculate the wide mesopore volumes (8 nm $< d <$ 50 nm) and the macropore ($d >$ 50 nm) volumes. Particle densities (ρ_p) were determined from the mercury displacement method.

The ultimate analyses (ash free) and the surface chemistry analysis of the ACs were carried out in a Perkin-Elmer (model 2400 CHN) analyzer, and by means of X-ray photoelectron spectroscopy (XPS) and Temperature Programmed Desorption (TPD), respectively. The XPS analyses of the samples were carried out using a 5700C model Physical Electronics apparatus with MgKα radiation (1253.6 eV). For the analysis of the XPS peaks, the C1s peak position was set at 284.5 eV and then used as a reference to locate the other peaks. The TPD profiles were obtained with a custom quartz tubular reactor placed inside an electrical furnace. The samples were heated from room temperature up to 900 °C at a heating rate of 5 °C/min in a helium flow (200 cm^3 STP/min). The amounts of CO and CO_2 desorbed from the samples were monitored with an ndir-analyzer Siemens (mod. Ultramat 22) apparatus. Scanning electron microscopy (SEM) was applied to study the microstructure of the ACs. The SEM micrographs were obtained by means of a model JSM 840 Jeol apparatus. The average sizes (radius R_p) of the ACs particles were estimated using an image analysis procedure.

2.2 Adsorption procedure

The organic compounds used as adsorbates (PA, BA, SA) have been supplied by Merck in the highest available purity. Table 1 shows some of their properties.

Table 1 Properties of the adsorbates

Adsorbates	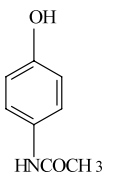 PA	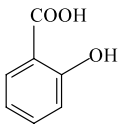 SA	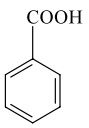 BA
Molecular weight (g/mol)	151.2	138.1	122.1
Molecular size (nm^2)	0.362	0.375	0.291
Melting point (°C)	168–172	158–161	121.5–123
Solubility (g/L)$^{20\,°C}$	14	1.8	2.9
pKa	9.9	2.98	4.2
Dipole moment (D)	2.81–5.86	2.40	1.72

The equilibrium and the kinetic tests have been carried out in an orbital incubator (Gallenkamp, model INR-250) at 180 rpm equivalent stirring rate. The temperature for the experiments varied between 283 K and 313 K. The aqueous solutions of the adsorbates were prepared with distilled water and different initial concentrations (PA: 0.050–0.600 mmol/L; BA and SA: 0.050–1.000 mmol/L). At these initial concentrations, the initial pH values were around 6 for PA, and they varied from 4.3 to 3.5 for BA, and from 4 to 3 for SA, approximately. For the equilibrium tests, samples of 100 mL and AC doses of 100 mg/L were put in contact in stoppered flasks. The contact times to reach the adsorption equilibriums varied between seven and ten days. For the kinetic tests, PA, BA and SA solutions (0.600 mmol/L) were also put in contact with adsorbent doses of 100 mg/L. The adsorbate concentrations were determined by UV spectroscopy at the following wavelengths: PA: $\lambda_{max} = 243$ nm; BA: $\lambda_{max} = 224$ nm; SA: $\lambda_{max} = 296$ nm. Because of the varying location of the wavelength for the peaks of absorbance as the pH of the aqueous medium changes, it was necessary in many cases, to set the samples at the pH range for which the spectrum does not vary or it does a little, and the calibration plots were rightly developed, according to the selected wavelength. This step of pH fitting has been carried out, when necessary, with HCl/NaOH at the dilution of the sample step, just before its UV analysis. A UV-Visible (Varian, model Cary 1E) spectrophotometer was used for the analyses. The effect of the pH on the amounts adsorbed in the equilibrium was studied at pH ranging from 2 to 12. The initial pH of the solutions was adjusted with HCl/NaOH (0.1 M).

The equilibrium concentrations of the adsorbate on the adsorbent phase q_e (e.g., in mmol/g of dry adsorbent) were calculated as:

$$q_e = \frac{C_o - C_e}{w} \quad (1)$$

where C_o and C_e represent the initial and equilibrium concentrations (e.g., in mmol/L) of the adsorbate in solution, respectively, and w is the adsorbent dose (g/L).

The existing concentrations on the solid phase (q_t, mmol/g) in the kinetic tests were calculated as:

$$q_t = \frac{C_o - C_t}{w} \quad (2)$$

where C_t (mmol/L) represents the adsorbate concentration in the liquid phase at time t (min).

3 Results and discussion

3.1 Characterization of the activated carbons

Physical and chemical characterizations of adsorbents are necessary to understand their different behaviours when put in contact with adsorbates. Eucalyptus kraft lignin is not a porous material ($A_{BET} < 1$ m^2/g) as supplied. It has no adsorption capacity as is. A thermochemical process including an activation step is necessary to develop any specific surface area. Then a high grade of porosity can take place. The physical properties and the burn offs of ACs—calculated (%) as the sample weight loss relative to completely devolatilized kraft lignin—are given in Table 2. The series includes ACs with low, intermediate, and high activation degrees. It can be observed a progressive increase in A_{BET} as the burn off increases. A4 characterization revealed that it is a typically microporous AC. Interesting values in the mesopore and macropore volumes, as well as high external surface areas, are noticeable in A12 and A20. Ultimate analyses of the ACs (Table 2) showed an increase in the total oxygen content as the burn off increased, in agreement with the preparation process.

TPD analysis provided information about the nature of the carbon-oxygen groups formed on the carbonized surface during CO_2 gasification. CO_2 desorbed amounts belong to the carboxylic acids and the lactones surface groups decomposition. CO desorption begins at higher temperatures than CO_2, and it is related to the decomposition of carbon-oxygen surface groups like phenol, ether, carbonyl and quinone. Anhydrides of carboxylic acids produce both CO_2 and CO molecules in their decomposition (Lizzio et al. 1990; Zielke et al. 1999). Table 3 displays the corresponding carbon-oxygen surface groups. It can be observed that the amounts that desorbed as CO_2 and CO were the highest for A20 indicating the most of oxygen complexes are formed as burn off increases during the partial gasification.

The chemical nature of the surfaces has been also studied by means of XPS. Table 4 shows the relative atomic concentrations of C1s and O1s in the ACs surface, the O/C surface atomic ratios, and for the sake of comparison, we

Table 2 Physical properties of the activated carbons

AC	A4	A12	A20
A_{BET} (m^2/g)	760	926	1049
A_S (m^2/g)	45.7	130.3	254.0
Burn off (%)	27.5	40.4	51.4
$V_{microp.CO_2}$ (cm^3/g)	0.267	0.307	0.326
$V_{microp.N_2}$ (cm^3/g)	0.312	0.384	0.413
$V_{mesop.}$ (cm^3/g)	0.099	0.236	0.398
$V_{macrop.}$ (cm^3/g)	0.026	0.044	0.081
ρ_p (g/cm^3)	0.579	0.483	0.417
R_p (μm)	6.50	3.54	3.78
Ultimate analysis (ash free)			
C (%)	95.5	94.9	94.3
H (%)	0.87	0.72	0.66
O (%)	3.63	4.38	5.04

Table 3 Amounts of CO_2, CO and carbon-oxygen groups from the areas under the TPD peaks

AC	mg_{CO_2}/g_{AC}	mg_{CO}/g_{AC}	carbon-oxygen groups on AC surface						
			carboxylic acid	lactone	anh. carbox. acid	phenol	ether	carbonyl	quinone
A4	7	10	1.12	5.88	–	0.95	1.73	2.29	5.03
A12	8	15	6.79	0.73	1.58	3.84	2.52	4.93	2.61
A20	9	21	7.51	0.86	2.48	1.93	4.98	6.80	5.44

Table 4 C and O surface contents from XPS analyses. Values in % of total atomic surface concentration

AC	C1s	O1s	surface (O/C) $\times 10^2$	bulk (O/C) $\times 10^2$
A4	92.82	7.18	7.74	3.80
A12	93.23	6.77	7.26	4.62
A20	85.47	14.53	17.0	5.35

have included the corresponding bulk values of the O/C ratio (weight) derived from ultimate analyses. Those values suggest that the carbon-oxygen surface groups formed during gasification are located mainly in the activated carbons surface. Table 5 presents the surface atomic concentration of the different surface groups, calculated from the XPS peaks deconvolution (Fig. 1), as well as their assignation and location in the spectra (Noll et al. 1992; Biniak et al. 1997). The morphology of the external surfaces was studied by SEM. They present cavities, cracks and irregular protrusions.

3.2 Adsorption isotherms

The adsorption isotherms are important to describe how solutes interact with adsorbents, which is fundamental in optimizing their use and modelling the adsorption systems. The adsorption isotherms of PA on A4, A12 and A20 at different temperatures are plotted in Fig. 2. In all the cases the highest adsorption capacity corresponded to A20. The adsorbed amounts grew when the AC burn off increased. This is in agreement with higher total surface areas, external areas and meso and macropore volumes. The amount of adsorbed PA diminishes when temperature decreases. This behaviour suggests an apparent endothermic nature of the adsorption process. The equilibrium isotherms of BA and SA on A20, at 293 K, 303 K, and 313 K, are plotted in Fig. 3. In these cases, the adsorbed amounts decline when temperature increases. This behaviour suggests an exothermic nature of the adsorption process.

The adsorption isotherms shown in Figs. 2–3 can be classified as type I of BDDT (Brunauer et al. 1940) as well as type L2 of Giles (Giles et al. 1960) classifications. Their shapes mean that there is no strong competition between the solvent and the solute to occupy the adsorbent surface sites. The isotherms for PA adsorption suggest that is possible to remove the adsorbate at low concentrations. The experimental data were fitted to Langmuir equation (Langmuir 1918):

$$q_e = \frac{KMC_e}{1 + KC_e} \tag{3}$$

where K is the Langmuir equilibrium constant, usually related to the enthalpy of adsorption, and M is the equilibrium concentration of adsorbate on the solid phase corresponding to a complete coverage (maximum adsorption capacity) of the available adsorption sites. These equation parameters were calculated using a non linear regression fitting procedure. The Langmuir constants (K in L/mmol; M in mmol/g) and χ^2 (average quadratic deviation) are also reported in Figs. 2–3. Related to PA adsorption on A4 (Fig. 2), it can be observed how the maximum adsorption capacity (M) at all temperatures increased approximately a 30 percent when the activation time was extended up to 12 h (A4 to A12). By contrast, the relative increment (A20/A12) was less than a 10 percent when the activation time grew from 12 to 20 h (A12 to A20). The improvements in M (%) values were close to those achieved in terms of the corresponding microporosity developments for the ACs (A4, A12 up to A20).

Moreover, it is of interest to compare the adsorption capacities among adsorbates. So, we can calculate, at any q_e value, the adsorbate equivalent surface area that would cover one gram of AC surface assuming that the solute molecules take a parallel orientation on the AC surface and the surface areas covered by each adsorbed molecule are: 0.362 nm^2 (PA), 0.375 nm^2 (SA) and 0.291 nm^2 (BA). The molecular sizes (width × depth) for them are: PA (0.877 × 0.413 nm); SA (0.703 × 0.533 nm); and BA (0.703 × 0.414 nm). Then the adsorbate equivalent surface areas are:

$$\begin{aligned}
A_{PA}(m^2_{PA}/g_{AC}) &= 218.0\ (m^2_{PA}/mmol_{PA}) \cdot q_e\ (mmol_{PA}/g_{AC}) \\
A_{SA}(m^2_{SA}/g_{AC}) &= 225.9\ (m^2_{SA}/mmol_{SA}) \cdot q_e\ (mmol_{SA}/g_{AC}) \\
A_{BA}(m^2_{BA}/g_{AC}) &= 175.3\ (m^2_{BA}/mmol_{BA}) \cdot q_e\ (mmol_{BA}/g_{AC})
\end{aligned} \tag{4}$$

As examples, Table 6 shows the values of the equivalent area occupied (4), as well as the corresponding adsorbate coverage factors (related to A_{BET}) at the solute concentration C_e: 0.400 mmol/L. The coverage factors for PA adsorption were quite similar; they depend little on temperature,

Table 5 Assignments of surface groups from XPS spectra. Values in % of total atomic surface concentration

AC	C1s				O1s		
	–C–C– 284.4 eV	C–O–C and/or C–OH 286.0 eV	C=O 288.5 eV	–COOH 290.8 eV	C–O–C and/or C–OH 533.0 eV	C=O 531.4 eV	H_2O chemisorbed 535.0 eV
A4	67.32	15.08	5.94	4.47	3.57	2.95	0.66
A12	66.75	15.08	6.59	4.79	2.92	2.78	1.07
A20	57.07	18.37	6.06	3.98	5.44	7.41	1.68

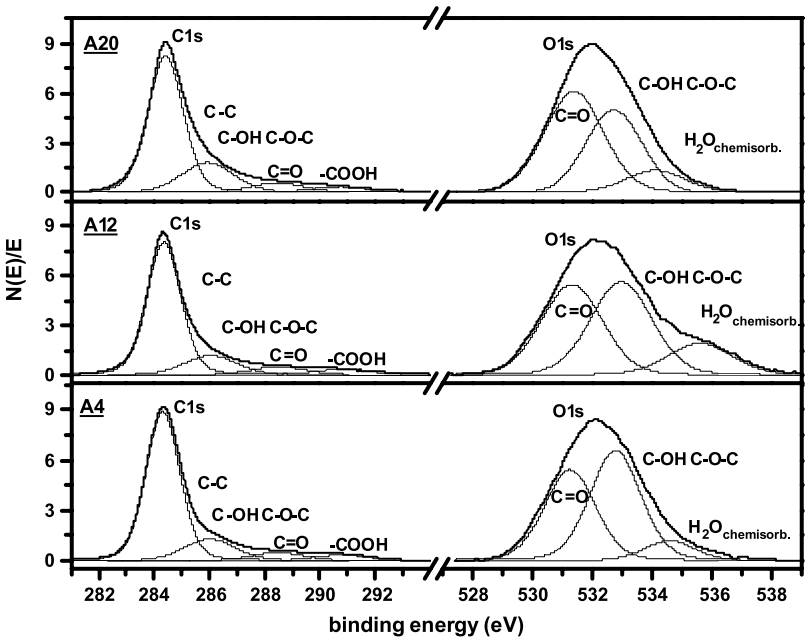

Fig. 1 XPS spectra deconvolution for the activated carbons

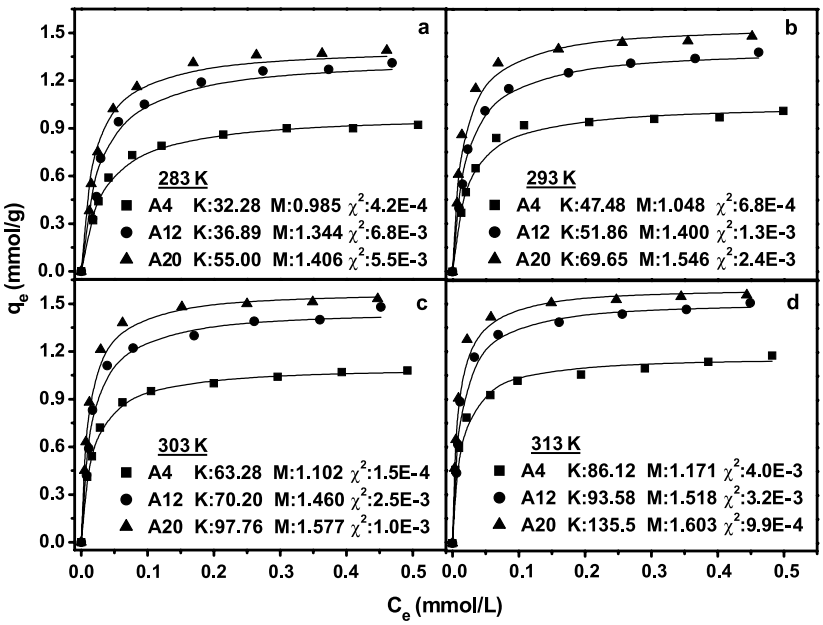

Fig. 2 Adsorption isotherms of PA on the different activated carbons: (**a**) 283 K, (**b**) 293 K, (**c**) 303 K, (**d**) 313 K. Experimental data (*dots*) and Langmuir fits (*curves*)

being less than 40 % in all the cases. The coverage factors values for SA and BA revealed moderate levels in the total surface taken, with decreasing yields as temperature rose.

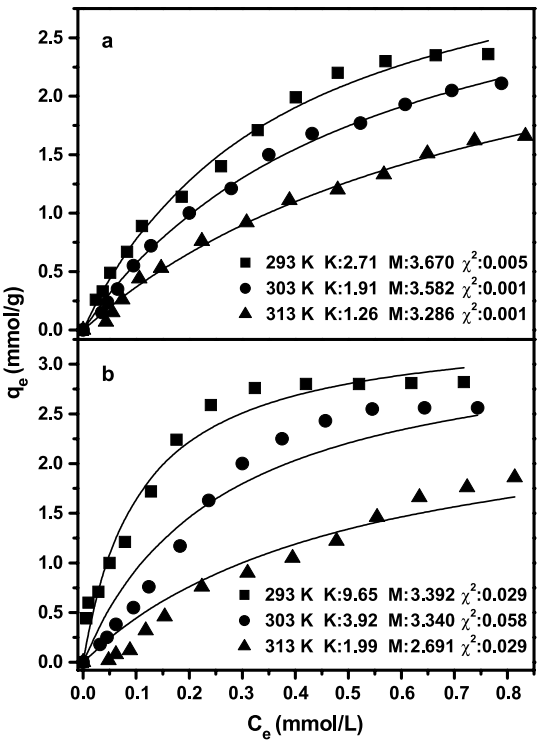

Fig. 3 Adsorption isotherms of (**a**) BA, (**b**) SA, on A20, at different temperatures. Experimental data (*dots*) and Langmuir fits (*curves*)

3.3 pH effect

The pH of the adsorbate solution has influence on the whole adsorption capacity, the surface charge and the ionization of the functional groups on the adsorbent, and the degree of ionization of the molecules in solution. H^+ and OH^- are usually strongly adsorbed, and therefore, the adsorption of other ions is affected by the solution pH. Frequently, anions can be easily adsorbed at low pH values, due to the presence of H^+ ions on the solid surfaces. At high pH values, cations are better adsorbed on the surfaces negatively charged.

Figure 4a plots the effect of pH on the adsorption of PA on A4, A12, and A20. Figure 4b corresponds to SA and BA on A20. In all the cases, no perceptible pH variations in the samples were observed during the adsorption processes. According to Fig. 4a, PA (pKa = 9.9) adsorption does not vary appreciably within the pH range studied. At high pH, the surface groups are anionic and they can present repulsion forces in opposition to the dissociated PA molecules. However, a significant adsorption of the anionic PA molecules on the ACs may occur at basic pH. Regardless, the adsorption capacity observed can be also explained taking into account the contribution of non electrostatic sorption mechanisms such as hydrogen bonds and other Van der Waals type forces. As it can be seen in Fig. 4b, the amount of SA adsorbed decreased with increasing pH. SA at low pH is almost undissociated (weak acid, pKa = 2.98). Under these conditions, chemical groups on the surface will present a decrease in net negative charge. As pH is becoming lower, the protons favour the formation of hydrogen bonds between the oxygen

Table 6 Equivalent surfaces of the adsorbed compounds (A) corresponding to C_e: 0.400 mmol/L; coverage factors; and thermodynamic results: ΔG, ΔH (kJ/mol); ΔS (J/mol K)

Adsorb.	AC	T (K)	A (m^2/g_{AC})	Cov. Fac.	ΔG	ΔH	ΔS
PA	A4	283	199.3	0.262	−24.4	23.8	170.4
		293	217.0	0.286	−26.2		
		303	231.1	0.304	−27.8		
		313	248.1	0.326	−29.5		
	A12	283	274.2	0.296	−24.7	22.8	167.9
		293	291.2	0.314	−26.4		
		303	307.3	0.332	−28.1		
		313	322.3	0.348	−29.8		
	A20	283	293.2	0.280	−25.7	22.3	169.2
		293	325.3	0.310	−27.1		
		303	335.2	0.320	−28.9		
		313	343.1	0.327	−30.7		
SA	A20	293	608.6	0.580	−22.3	−60.2	−129.6
		303	460.7	0.439	−20.8		
		313	269.4	0.257	−19.7		
BA	A20	293	334.6	0.319	−19.2	−29.1	−33.4
		303	272.0	0.259	−19.0		
		313	193.0	0.184	−18.6		

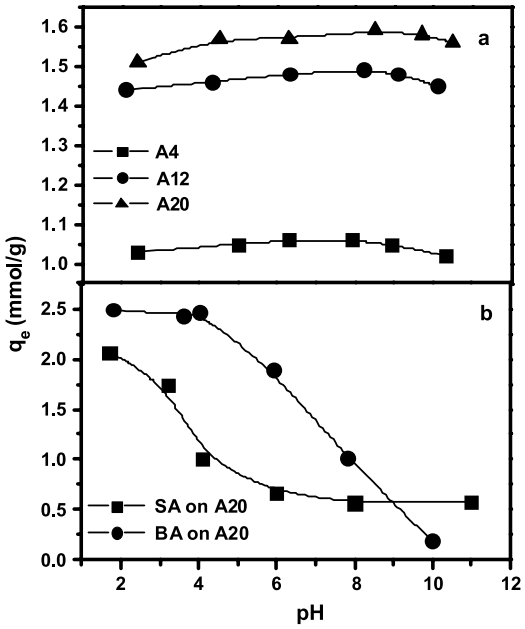

Fig. 4 pH effect on the adsorption equilibrium at 293 K (C_o: 0.600 mmol/L): (**a**) PA on A4, A12 and A20, (**b**) BA and SA on A20

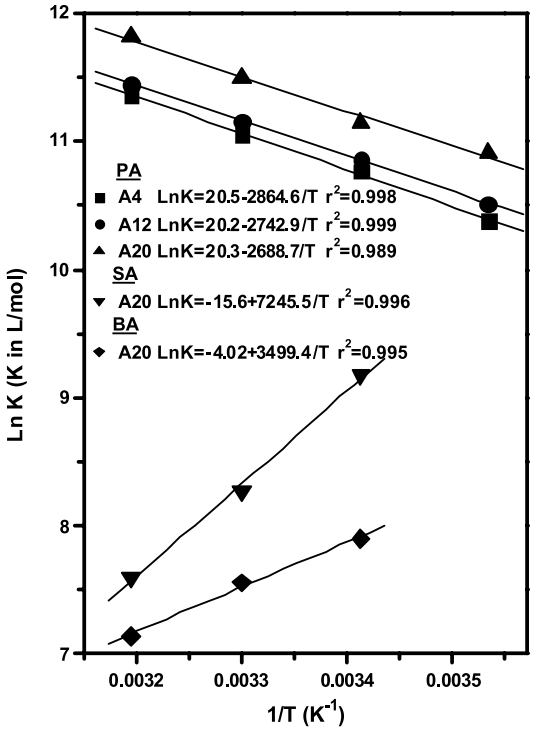

Fig. 5 Plots for the adsorption enthalpies

of SA and the surface of the AC (rich in oxygen-groups), thereby the adsorption is favoured. At high pH, the degree of SA dissociation and the number of sites negatively charged on the AC are increased. So, forces of repulsion between the salicylates and the surface can occur, making difficult the adsorption process. Figure 4b also shows the adsorbed amount of BA (pKa = 4.2) with a decrease in adsorption as pH increases. It is due to the grade of the acid dissociation; like the same effect which has been described for SA.

3.4 Thermodynamic study

The thermodynamic approach to the adsorption analysis provides information about the process ability to take place and the stability of the adsorbed phase as well. The temperature is a variable with influence on the solubility of the solutes and the adsorbed state as well. An increase in temperature generally improves the solubility of the molecules and their diffusion within the pores of the ACs. The change in temperature produces a displacement from or towards the adsorbed phase.

The changes on the free energy (ΔG), enthalpy (ΔH), and entropy (ΔS) of the adsorption processes of PA, SA and BA were calculated using the following equations:

$$\Delta G = -RT \ln K \tag{5}$$

$$\frac{\partial \ln K}{\partial T} = \frac{\Delta H}{RT^2} \Rightarrow \ln K = \ln K_o - \frac{\Delta H}{RT} \tag{6}$$

$$\ln K_o = \frac{\Delta S}{R} \tag{7}$$

where R is the universal gases constant (8.314 J/mol K), T is the absolute temperature (K), and K_o is the preexponential factor, i.e., K value when T tends to infinite. Once the Langmuir constant is determined, the adsorption process dependency on the temperature can be studied. The values of ΔG, ΔH and ΔS obtained are given in Table 6. The values of ΔH have been estimated by applying the Van't Hoff equation, which in its logarithmic form can be written as (6). If ΔH depends quite little on temperature, (6) becomes a straight line when plotting $\ln K$ versus $1/T$. According to the plots obtained (Fig. 5), the values of ΔH have been determined from the slopes (6), and ΔS from the intercepts (7). The determination coefficients (r^2) were acceptable for all ACs and all adsorbates studied. The adsorbed amounts of PA rose as temperature increased. To understand this phenomenon one can consider the variation in the aggregating state that the molecules of adsorbate can present in aqueous solution. Terzyk et al. (2003) reported the formation of dimers (oligomers) of PA in aqueous solutions, favoured at acid media. If the molecules of PA can form micelles or ionic aggregates, and they are the prevalent forms at the existing conditions, then, the aggregation effect can imply a high difficulty to the penetration into the micropores and the narrow mesopores. If the dimers formation is of endothermic character; therefore, it results in a greater adsorption capacity when temperature increases. This results in a net endothermic nature of the adsorption processes. By contrast, the adsorbed amounts of SA and BA rose as the temperature decreased;

this suggests the net exothermic nature of their adsorption processes. The negative values of ΔG indicate the feasibility and spontaneity of the adsorption processes studied. On the other hand, K_o can be related to the entropy change (7) by combining the Gibbs-Helmholtz ($\Delta G = \Delta H - T\Delta S$) equation, the Van't Hoff's (6), and the equilibrium constant related to the free energy equation (5). The positive values of the adsorption entropy changes for PA are coherent with a lower grade of freedom of the molecules in the fluid phase than in the adsorbed state, what also means that the adsorption processes induce a higher degree of randomness in the spontaneous systems. In these cases ($\Delta H > 0$; $\Delta S > 0$), the processes only occur when $T\Delta S > \Delta H$. So, the benefit of the positive entropy change has to exceed the endothermic effect of the process. It is necessary that T becomes enough high. If not, the process will not be thermodynamically allowed. So, the T minimum values for A4, A12 and A20 are 139.7; 135.8; and 131.8 K, respectively. On the other hand, the negative values of ΔS for SA and BA in the exothermic processes result in a lower grade of freedom of the molecules in the adsorbed phase than in the fluid phase. In these cases ($\Delta H < 0$; $\Delta S < 0$), the process can only occur when $|T\Delta S| < |\Delta H|$. The processes have to become exothermic enough to overtake the disadvantage due to the negative change of entropy. If the temperature value is enough high, the term $T\Delta S$ can surpass the term ΔH, and the process does not take place. So, the highest value of T for SA adsorption according to a spontaneous process results in 464.5 K; the upper value for BA is 871.3 K. However, it is necessary to remind that the estimated ΔG, ΔH and ΔS values represent the apparent behaviours associated with the processes at the experimental conditions set.

3.5 Comparative study among adsorbates

The three organic compounds selected have slightly different molecular size and weight, but the solubility in water is much higher for the nitrogen compound, i.e., paracetamol.

Liquid-phase adsorption can be analyzed in physical and chemical terms. In general, large molecules are fixed better, although it can be controlled by their size and the narrow porosity of the adsorbent. Regarding the solubility in water, compounds with low solubility have, frequently, a high affinity toward the active carbon surface. Usually, a molecule with low polarity is better adsorbed from its aqueous solution than another with high polarity; this is because the former does not need to overcome the solvent-adsorbate interactions. On the other hand, the polarity benefits the interactions with the functional groups on the surface of the ACs (Radovic and Rodríguez-Reinoso 1996; Radovic et al. 2000).

Moreover, the aromatic compounds adsorption implies the formation of electron donor-acceptor complex systems

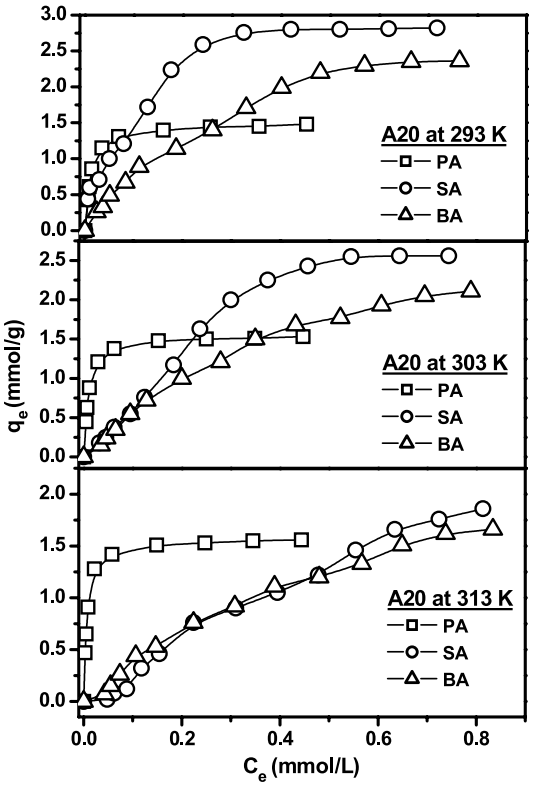

Fig. 6 Isotherms for comparison among adsorbates at different temperatures

between the carbon-oxygen functional groups of the adsorbent surface, which act as donors and the π electron system of the aromatic ring in the adsorbate molecule, which acts as an acceptor. The presence of groups with electronegative character in the aromatic ring favours the formation of the interaction; thus the aromatic ring will act as an acceptor if the electronic cloud moves towards such substitutes. In addition to this, other interactions can also contribute to adsorption; the hydrophobic and hydrogen bonds. In all the cases, the resulting macroscopic adsorption behaviours are usually complex combinations of many interacting phenomena with electrostatic and Van der Waals type forces, and to separate these effects is difficult.

To arrange a comparative study among the adsorption capacity of the adsorbates, we have analyzed the adsorption isotherms for A20 at three different temperatures, as displayed in Fig. 6. As it has been said, related to PA, the adsorption capacity of A20 was very high at low solute concentrations (high affinity isotherms), and it increased with temperature (apparent endothermic character). PA has the highest dipole moment. In contrast to PA, the capacities for SA and BA adsorption were increasing progressively for their higher concentrations and the lower temperatures (exothermic behaviour). At high solute concentration, SA was the adsorbate preferably removed. It is in accordance

with a higher dipole moment for the SA molecule. The following is a brief analysis for each one of the adsorbates:

Carboxylic acids in aqueous solutions usually present a dimer state by formation of two hydrogen bonds between the hydroxyl group of one molecule and the carbonyl group of another. BA can self-associate easily, and their species would access to microporosity with difficulty. In any case, if BA is as a monomer, then the electrons involved in the formation of bonds, tend to be more attracted to the oxygen (higher electronegativity). This effect produces a weak electronic lack in the carbon of the carboxylic group, which the atom tries to compensate by attraction of the electrons participating in the bond that connect with the carbon of the benzene ring. In this case, the aromatic ring will behave as an electron acceptor from the groups on the carbon surface, which will act as donors. SA is an *o*-substituted acid and the adjacent groups can interact directly by hydrogen bonds. SA is easily adsorbed. SA is also the least soluble and its benzene ring, such as BA, behaves as an electron acceptor, which induces a good affinity toward the activated carbon surface. In PA, –NHR and –OH groups are electron-donors to the aromatic ring, which confer low affinity to the aromatic ring toward the adsorbent surface. PA is the most soluble and dipole-dipole interactions with the solvent can be also produced.

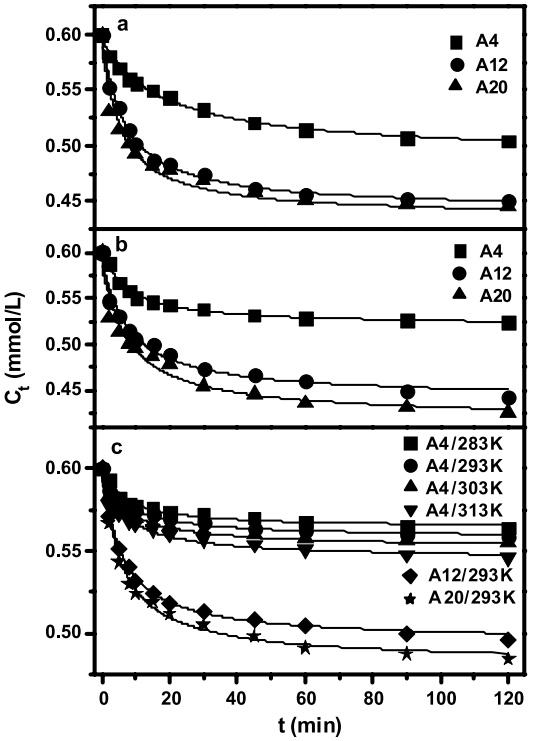

Fig. 7 Kinetics of (**a**) BA at 293 K, (**b**) SA at 293 K, (**c**) PA adsorption at different temperatures. C_o: 0.600 mmol/L; w: 0.100 g/L. Experimental data (*dots*) and fits (*curves*, (8))

3.6 Kinetic study

Both, the equilibrium and the kinetic results help to measure the yield and the rate of the adsorption process. In the present work, in order to arrange the data, we have considered the kinetic studies in terms of to achieve an empirical equation to reproduce the concentration decline curve for each experiment, and to estimate the effective diffusion coefficients, assuming the intraparticle mass transfer as the rate-controlling step. Figure 7 shows the kinetics of PA, SA and BA adsorption on the ACs at different temperatures. A sharp decrease in the adsorption rate is observed for the first minutes of contact time. This step corresponds to a fast coverage of the surface in the widest pores and the most active sites. A second step develops for half an hour approximately with an intermediate decreasing rate. This step is the most interesting to the kinetic control for its relation to the narrow mesopores and micropores coverage. The last part ends at the equilibrium conditions, after several days of contact time. The adsorption rate of PA on A4 at non-equilibrium contact times increased with temperature, indicating the activating effect of this variable (Fig. 7c). This is a result of the increase in the mobility of the molecules as well as an improvement in the mass transfer parameters. When ACs are compared, the rate observed grew as burn off increased, as a consequence of the better developed macro and mesoporosities. After 120 minutes of contact time, the grades of approach to the adsorption equilibrium were higher than a 70 percent for SA, BA and PA (A12 and A20). In the systems of PA on A4, the values at all temperatures were less than a 50 percent. It is due to the intraparticle diffusivity control for the PA molecule transfer through the net of the microporosity that gives internal shape to A4.

An empirical model, exponential type, has been used to fit the experimental results:

$$C_t = a \exp\left(\frac{b}{c+t}\right) \tag{8}$$

where a, b and c are empirical coefficients. Those are summarized in Table 7. It includes the experimental q_e values for each test, as well as the χ^2 (average quadratic deviation) values.

Referred to the mass transfer models, a great number of them have been proposed, which differ in their description of the diffusion processes occurring within the porous particle. In the present study, we have considered the solid homogeneous sphere diffusion model (HSDM), with a constant internal diffusivity (D_i) across the radial position (r) in the particle. The equation is:

$$\frac{\partial q(r)}{\partial t} = \frac{D_i}{r^2}\frac{\partial}{\partial r}\left[r^2\frac{\partial q(r)}{\partial r}\right] \tag{9}$$

Table 7 Fitting parameters from (8) for kinetics; C_o: 0.600 mmol/L; w: 0.100 g/L; T (K); q_e (mmol/g); a (mmol/L); b, c (min)

Adsorb.	PA						SA			BA		
AC	A4				A12	A20	A4	A12	A20	A4	A12	A20
T	283	293	303	313	293	293	293	293	293	293	293	293
a	0.564	0.558	0.552	0.545	0.495	0.482	0.520	0.441	0.419	0.491	0.442	0.436
b	0.408	0.502	0.573	0.666	1.196	1.439	1.118	2.610	3.091	3.753	2.312	1.998
c	6.579	7.174	7.263	7.594	6.243	6.662	7.667	8.871	9.266	19.49	7.703	6.613
χ^2	2.1E−6	1.7E−6	3.4E−6	8.1E−6	2.4E−6	7.5E−6	4.2E−6	4.0E−5	1.0E−4	6.8E−6	1.0E−5	6.0E−6
q_e	0.920	1.010	1.080	1.180	1.380	1.480	0.875	2.000	2.760	1.200	1.500	1.990

Crank (1956) developed the following equation for spherical particles with radius R_p:

$$\frac{q_t}{q_e} = 1 - \frac{6}{\pi^2}\sum_{n=1}^{\infty}\frac{1}{n^2}\exp\left(-\frac{D_i n^2 \pi^2 t}{R_p^2}\right) \tag{10}$$

This provides an exact solution for the situation often called "infinite bath"; i.e., a constant concentration of solute around the solid surface and a negligible external film resistance. For "short times" (S_t), or more precisely: $q_t/q_e < 0.3$, (10) is quite close to:

$$D_{St} = \left(\frac{q_t}{q_e}\right)^2 \frac{\pi R_p^2}{36t} \tag{11}$$

For "long times" (L_t), the higher terms in Crank's series solution become extremely small, and only the first term has prevalence. We have:

$$D_{Lt} = \frac{R_p^2}{\pi^2 t}\ln\left[\frac{6/\pi^2}{1-(q_t/q_e)}\right] \tag{12}$$

Due to mathematical reasons, D_{Lt} values only may be positive from $(q_t/q_e) > [1-(6/\pi^2) \approx 0.392]$. In the present work, we have used (11) and (12) to determine the D_i values (D_{St} and/or D_{Lt}) in the kinetic runs from Fig. 7. The average sizes (radius) of the ACs particles are reported in Table 2. The q_t values were supplied by the exponential model (8).

Figures 8 and 9 plot the effective diffusivity values for PA, and BA and SA adsorption, respectively, in terms of the increasing surface coverage (q_t). The equations did not predict constant values. After an initial growth that we can relate to a necessary minimum coverage to set the surface diffusion mechanisms, we have obtained decreasing apparent diffusion coefficients according to an increasing difficulty for the molecules to penetrate into the porous structures. As the adsorption phenomenon occurs (long times), the mouth of the pores can be partially obstructed. The surface areas of the pores are gradually less available for adsorption. It is well observed in the A4 trends. The highest values corresponded to the microporous A4 and "short times" in several cases for BA and SA. They are direct results from the particular profiles of (q_t/q_e) functions, which affect (11) and (12), which are, on the other hand, highly according to R_p values; being the highest one for A4. At the same time, at intermediate coverage values, the wider developed mesoporosity (A12 and A20) can influence the results. In any case, the sharp decreases in D values at long contact times evidences well enough a step with strong intraparticle diffusion control, previous to adsorption.

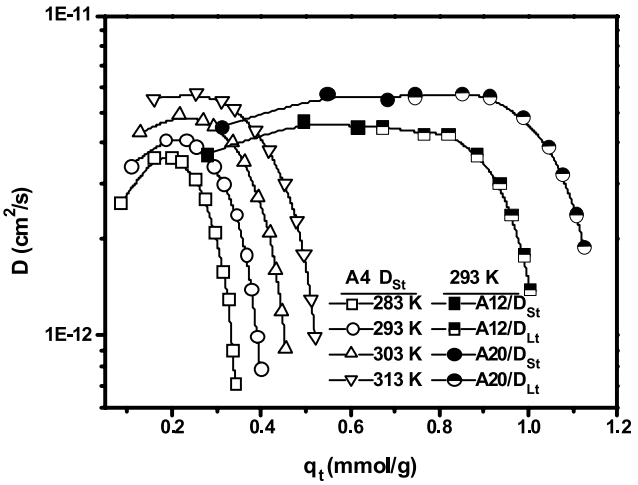

Fig. 8 Effective diffusion coefficients for PA. C_o: 0.600 mmol/L; w: 0.100 g/L

4 Conclusions

Activated carbons obtained from lignin, at different experimental conditions, have been successfully employed as adsorbents for PA, BA and SA removal in aqueous phase.

The adsorption equilibrium data were fitted to the Langmuir isotherm for all the activated carbons. It has been found that the activated carbons burn-off influences on the adsorption capacity. Moreover, the adsorption results revealed

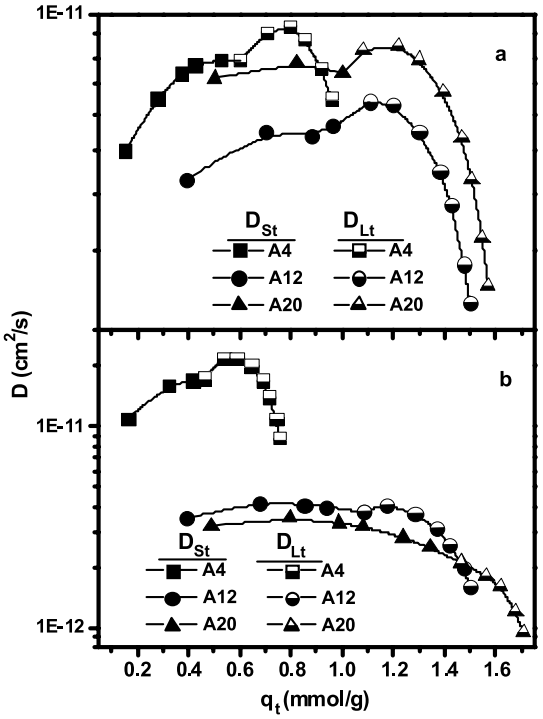

Fig. 9 Effective diffusion coefficients. C_o: 0.600 mmol/L; w: 0.100 g/L; T: 293 K: (**a**) BA, (**b**) SA

strong dependence on the pH of the medium in BA and SA systems.

The thermodynamic analysis indicated that the adsorption was spontaneous and endothermic for PA; exothermic for BA and SA. The forces involved in the adsorption energies were low, like the Van der Waals types.

The experimental kinetic values were fitted to a simple exponential equation. The effective diffusion coefficients in the range from 10^{-12} to 10^{-11} cm^2/s suggested that the mass transfer through the internal porosity became the controlling step.

Despite the interesting adsorption yields obtained, further investigations should be carried out in the chemical, engineering, and economic fields, before the tested activated carbons reach applications at a large scale. For example, expanded studies with multisolute samples would be developed at laboratory/pilot plant scale, previous to applications of the adsorbents in industrial separations with purification/environmental purposes. Cost studies derived from the used adsorbent management and the energy involved would be considered as well.

Acknowledgements The authors acknowledge to the Spanish DGICYT (Dirección General de Investigación Científica y Técnica)-MEC (Ministerio de Educación y Ciencia, Proyecto CTQ-2006/11322) and the Junta de Andalucía (PAI-TEP184) for the financial support.

References

Ania, C.O., Parra, J.B., Pis, J.J.: Effect of texture and surface chemistry on adsorptive capacities of activated carbons for phenolic compounds removal. Fuel Process. Technol. **77–78**, 337–343 (2002a)

Ania, C.O., Parra, J.B., Pis, J.J.: Influence of oxygen-containing functional groups on active carbon adsorption of selected organic compounds. Fuel Process. Technol. **79**, 265–271 (2002b)

Ayranci, E., Duman, O.: Adsorption of aromatic organic acids onto high area activated carbon cloth in relation to wastewater purification. J. Hazard. Mater. B **136**, 542–552 (2006)

Ayranci, E., Hoda, N., Bayram, E.: Adsorption of benzoic acid onto high specific area activated carbon cloth. J. Colloid Interface Sci. **284**, 83–88 (2005)

Biniak, S., Szymanski, G., Siedlewski, J., Swiatkowski, A.: The characterization of activated carbons with oxygen and nitrogen surface groups. Carbon **35**, 1799–1810 (1997)

Brasquet, C., Subrenat, E., Le Cloirec, P.: Selective adsorption on fibrous activated carbon of organics from aqueous solution: correlation between adsorption and molecular structure. Water Sci. Technol. **35**, 251–259 (1997)

Brunauer, S., Deming, L.S., Deming, W.E., Teller, E.: On a theory of van der Waals adsorption of gases. J. Am. Chem. Soc. **62**, 1723–1732 (1940)

Cotoruelo, L.M., Marqués, M.D., Rodríguez-Mirasol, J., Cordero, T., Rodríguez, J.J.: Adsorption of aromatic compounds on activated carbons from lignin: kinetic study. Ind. Eng. Chem. Res. **46**, 2853–2860 (2007a)

Cotoruelo, L.M., Marqués, M.D., Rodríguez-Mirasol, J., Cordero, T., Rodríguez, J.J.: Adsorption of aromatic compounds on activated carbons from lignin: equilibrium and thermodynamic study. Ind. Eng. Chem. Res. **46**, 4982–4990 (2007b)

Crank, J.: The Mathematics of Diffusion. Clarendon Press, Oxford (1956)

Franz, M., Arafat, H.A., Pinto, N.G.: Effect of chemical surface heterogeneity on the adsorption mechanism of dissolved aromatics on activated carbon. Carbon **38**, 1807–1819 (2000)

Giles, C.H., MacEwan, T.H., Nakhwa, S.N., Smith, D.: Studies in adsorption. Part XI. A system of classification of solution adsorption isotherms, and its use in diagnosis of adsorption mechanisms and in measurement of specific surface areas of solids. J. Chem. Soc. 3973–3993 (1960)

González-Serrano, E., Rodríguez-Mirasol, J., Cordero, T., Rodríguez, J.J.: Development of porosity upon chemical activation of kraft lignin with $ZnCl_2$. Ind. Eng. Chem. Res. **36**, 4832–4838 (1997)

Khenniche, L., Aissani, F.: Characterization and utilization of activated carbons prepared from coffee residue for adsorptive removal of salicylic acid and phenol: kinetic and isotherm study. Desalin. Water Treat. **11**, 192–203 (2009)

Koh, M., Nakajima, T.: Adsorption of aromatic compounds on C_xN-coated activated carbon. Carbon **38**, 1947–1954 (2000)

Langmuir, I.: The adsorption of gases on plane surfaces of glass, mica and platinum. J. Am. Chem. Soc. **40**, 1361–1403 (1918)

Lizzio, A.A., Jiang, H., Radovic, L.R.: On the kinetics of carbon (char) gasification: reconciling models with experiments. Carbon **28**, 1–9 (1990)

Márquez-Montesino, F., Cordero, T., Rodríguez-Mirasol, J., Rodríguez, J.J.: Powdered activated carbon from pinus caribaea sawdust. Sep. Sci. Technol. **36**, 3191–3206 (2001)

Mazet, M., Farkhani, B., Baudu, M.: Influence of heat or chemical treatment of activated carbon onto the adsorption of organic compounds. Water Res. **28**, 1609–1617 (1994)

Noll, K.E., Gounaris, V., Hou, W.: Adsorption Technology for Air and Water Pollution Control. Lewis Pub., Chelsea (1992)

Oda, H., Kishida, M., Yokokawa, C.: Adsorption of benzoic acid and phenol from aqueous solution by activated carbons-effect of surface acidity. Carbon **19**, 243–248 (1981)

Otero, M., Zabkova, M., Rodrigues, A.E.: Comparative study of the adsorption of phenol and salicylic acid from aqueous solution onto nonionic polymeric resins. Sep. Purif. Technol. **45**, 86–95 (2005)

Radovic, L.R., Rodríguez-Reinoso, F.: Carbon materials in catalysis. In: Thrower, P.A. (ed.) Chemistry and Physics of Carbon, vol. 25. Marcel Dekker, New York (1996)

Radovic, L.R., Moreno-Castilla, C., Rivera-Utrilla, J.: Carbon materials as adsorbents in aqueous solutions. In: Radovic, L.R. (ed.) Chemistry and Physics of Carbon, vol. 27. Marcel Dekker, New York (2000)

Rodríguez-Mirasol, J., Cordero, T., Rodríguez, J.J.: Preparation and characterization of activated carbon from eucalyptus kraft lignin. Carbon **31**, 87–95 (1993a)

Rodríguez-Mirasol, J., Cordero, T., Rodríguez, J.J.: Activated carbons from CO_2 partial gasification of eucalyptus kraft lignin. Energy Fuels **7**, 133–138 (1993b)

Shirgaonkar, I.Z., Joglekar, H.S., Mundale, V.D., Joshi, J.B.: Adsorption equilibrium data for substituted phenols on activated carbon. J. Chem. Eng. Data **37**, 175–179 (1992)

Tancredi, N., Cordero, T., Rodríguez-Mirasol, J., Rodríguez, J.J.: Activated carbons from uruguayan eucalyptus wood. Fuel **75**, 1701–1706 (1996)

Terzyk, A.P., Rychlicki, G., Biniak, S., Lukaszewicz, J.P.: New correlations between the composition of the surface layer of carbon and its physicochemical properties exposed while paracetamol is adsorbed at different temperatures and pH. J. Colloid Interface Sci. **257**, 13–30 (2003)

Zielke, U., Hüttinger, K.J., Hoffman, W.P.: Surface-oxidized carbon fibers: I. Surface structure and chemistry. Carbon **34**, 983–999 (1999)